Asian Research Journal of Mathematics
2(1): 1-15, 2017; Article no.ARJOM.30730

SCIENCEDOMAIN *international*
www.sciencedomain.org

Chemical Reaction Effects on MHD Nanofluid Flow of a Convection Slip in a Saturated Porous Media Over a Radiating Stretching Sheet with Heat Source/Sink

Srinivas Maripala[1*] and N. Kishan[2]

[1]Department of Mathematics, Sciences and Humanities, Sreenidhi Institute of Science and Technology, Yamnampet, Ghatkesar, Rangareddy District, Telangana-501301, India.
[2]Department of Mathematics, University College of Science, Osmania University, Hyderabad, Telangana 50007, India.

Authors' contributions

Both authors collaborated to bring this work into reality. Author NK identified the problem. Author SM designed the study, performed the mathematical analysis and wrote the first draft of the manuscript, managed the analyses, edited the study and worked on the literature. Both authors read and approved the final manuscript.

Article Information

DOI: 10.9734/ARJOM/2017/30730
Editor(s):
(1) Andrej V. Plotnikov, Department of Applied and Calculus Mathematics and CAD, Odessa State Academy of Civil Engineering and Architecture, Ukraine.
Reviewers:
(1) Sami Ullah Khan, International Islamic University, Pakistan.
(2) Mohammad Yaghoub Abdollahzadeh Jamalabadi, Dongguk University, Korea.
Complete Peer review History: http://www.sciencedomain.org/review-history/17422

Original Research Article

Received: 28th November 2016
Accepted: 27th December 2016
Published: 3rd January 2017

Abstract

Numerical analysis is presented to investigate the chemical reaction effects on magnetohydrodynamics convection slip flow of nanofluid in a saturated porous media over a radiating stretching sheet with heat source/sink. The model used for the nanofluid incorporates the effects of Brownian motion and thermophoresis. The governing boundary-layer equations of the problem are formulated and transformed into a non-similar form. The resultant equations are then solved numerically using finite difference method along with Thomas algorithm. The results are analyzed for the effect of different physical parameters on the dimensionless velocity, temperature and nanoparticle concentration fields and are presented through graphs.

**Corresponding author: E-mail: maripalasrinu@gmail.com;*

Keywords: MHD; chemical reaction parameter; heat source/sink; thermophoresis parameter; Brownian motion parameter; convection-radiation parameter; hydrodynamic (momentum) slip parameter.

1 Introduction

Interaction of nanoparticles in a fluid is called nanofluid. The nanoparticle used in nanofluid are normally composed of materials, carbides or carbon nanotubes, water, ethylene, glycol and oil which are common examples of based fluids. Nanofluid have their major applications in heat transfer. They demonstrate enhanced thermal conductivity and convective heat transfer coefficient, counter balance to the base fluid. A comprehensive study of convective transport in nanofluids was made by Buongiorno and Hu [1] and Buongiorno [2]. Dulal Pal and Netai Roy [3] studied the Lie Group Transformation on MHD Radiative Dissipative Casson Nanofluid Flow Over a Vertical Non-Linear, Stretching Surface with Non-Uniform Heat Source/Sink and Chemical Reaction. MYA Jamalabadi [4] studied the Entropy generation in boundary layer flow of a micro polar fluid over a stretching sheet embedded in a highly absorbing medium. A. A. Afify,M. J. UddinM. Ferdows [5], studied the Scaling group transformation for MHD boundary layer flow over permeable stretching sheet in presence of slip flow with Newtonian heating effects. Theories and experiments of thermal convection in porous media and state-of-the-art reviews, with special emphasis on practical applications have been presented in the recent books by Vafai [6], Pop and Ingham[7] and Bejan et al. [8]. Nanofluid transport in porous media has developed into a substantial area of research in recent years. This has been motivated by the thermally enhancing properties of nanofluids (Choi [9]) which are achieved owing to the presence of metallic nanoparticles suspended in base fluids (water, oil, etc.). In most of the chemical engineering processes, there is a chemical reaction between a foreign mass and the fluid. These processes take place in numerous industrial applications such as manufacturing of ceramics, food processing and polymer production [10]. Muthucumaraswamy [11] studied the effects of chemical reaction on vertical oscillating plate with variable temperature whereas Muthucumaraswamy and Manivannan [12] investigated first order chemical reaction on isothermal vertical oscillating plate with variable mass diffusion. Chamkha and Issa [13] investigated chemical reaction, heat generation or absorption effects on MHD boundary layer flow over a permeable stretching surface. Srinivas Maripala, Kishan. N [14], studied the unsteady MHD flow and heat transfer of nanofluid over a permeable shrinking sheet with thermal radiation and chemical reaction" However, such studies for nanofluid are rarely available in the literature especially when conjugate effects of heat and mass transfer are considered [15]. Srinivas Maripala and Kishan naikoti [16,17] studied the MHD effects on micropolar nanofluid flow over a radiative stretching surface with thermal conductivity. Dessie and Kishan [18] studied the heat transfer over stretching sheet embedded in porous medium with variable viscosity, viscous dissipation and heat source/sink. The above literature survey reveals that all of these studies are restricted to isothermal or isoflux boundary conditions. The use of the thermal convective boundary condition in order to study Blasius flow over a flat plate was first introduced by Aziz [19]. After his pioneering work, several authors used this boundary condition to study transport phenomena. Examples include N. Ali et al. [20-23], and Kishan and kavitha [24]. In all of the above studies, conventional no-slip boundary condition was used at the surface. Recently, Srinivas Maripala and Kishan Naikoti [25] studied the, MHD convection slip flow of a thermosolutal nanofluid in a saturated porous media over a radiating stretching sheet with heat source/sink when chemical reaction parameter is absent. In the present investigation is to study the chemical reaction effects of magnetohydrodynamics convection slip flow of a thermosolutal nanofluid in a saturated porous media over a radiating stretching sheet with heat source/sink. The governing equations are solved by using the implicit finite difference scheme using along with the Gauss-Siedel iteration method. The C-programming code is used to compute the values for the same.

2 Governaning Nanofluid Transport Model

The two-dimensional regime with a coordinate system with the $\bar{x}$ -axis aligned horizontally and the $\bar{y}$-axis is normal to it. A transverse magnetic field B_0 acts normal to the bounding surface. The magnetic Reynolds number is small so that the induced magnetic field is effectively negligible when compared to the applied magnetic field. We neglect the electric field associated with the polarization of charges and Hall effects. It is further assumed that the left of the plate is heated by the convection from the hot fluid of temperature

T_f(>T_w>T_∞) which provides a variable heat transfer coefficient $h_f(\bar{x})$. Consequently, a thermal convective boundary condition arises. It is further assumed that the concentration in the left of the plate C_f is higher than that of the plate concentration and free stream concentration C_∞ which provides a variable mass transfer coefficient $h_m(\bar{x})$. As a result, a mass convective boundary condition arises. The Oberbeck- Boussinesq approximation is utilized and the four field equations are the conservation of mass, momentum, thermal energy and the nanoparticles volume fraction. These equations can be written in terms of dimensional forms, extending the formulations of Buongiorno [26] and Makinde and Aziz [27]:

$$\frac{\partial \bar{u}}{\partial \bar{x}} + \frac{\partial \bar{v}}{\partial \bar{y}} = 0 \tag{1}$$

$$\rho_f(\bar{u}\frac{\partial \bar{u}}{\partial \bar{x}} + \bar{v}\frac{\partial \bar{u}}{\partial \bar{y}}) = \mu\frac{\partial^2 \bar{u}}{\partial \bar{y}^2} - \frac{\mu}{Kp}\bar{u} - \sigma {B_0}^2 \bar{u}, \tag{2}$$

$$\bar{u}\frac{\partial T}{\partial \bar{x}} + \bar{v}\frac{\partial T}{\partial \bar{y}} = \alpha\frac{\partial^2 T}{\partial \bar{y}^2} + \tau\left\{D_B\frac{\partial C}{\partial \bar{y}}\frac{\partial T}{\partial \bar{y}} + \left(\frac{D_T}{T_\infty}\right)\left(\frac{\partial T}{\partial \bar{y}}\right)^2\right\} - \frac{1}{\rho_f c_f}\frac{\partial q_r}{\partial \bar{y}} + \frac{Q_0}{(\rho c)_f}(T - T_\infty) \tag{3}$$

$$\bar{u}\frac{\partial C}{\partial \bar{x}} + \bar{v}\frac{\partial C}{\partial \bar{y}} = D_B\frac{\partial^2 C}{\partial \bar{y}^2} + \left(\frac{D_T}{T_\infty}\right)\frac{\partial^2 T}{\partial \bar{y}^2} - k_c(C - C_\infty) \tag{4}$$

The appropriate boundary conditions are following Datta [28] and Karniadakis et al. [29].

$$\bar{u} = \bar{u}_w + \bar{u}_{slip}\ ;\ \bar{v} = 0,\ -k\frac{\partial T}{\partial \bar{y}} = h_f(T_f - T\ ),\ -D_B\frac{\partial C}{\partial \bar{y}} = h_m(C_f - C\ )\ \text{at}\ \bar{y} = 0, \tag{5}$$

$\bar{u}$ tends to 0, T tends to T_∞, C tends to C_∞ as $\bar{y}$ tend to ∞

Here $\alpha = k/(\rho c)_f$ thermal diffusivity of the fluid; $\tau = (\rho c)_\rho / (\rho c)_f$, ratio of heat capacity of the nanoparticle and fluid; Kp: permeability of the medium; ($\bar{u}$, $\bar{v}$): velocity components along $\bar{x}$ and $\bar{y}$ axes, $\bar{u}_w = U_r(\bar{x}/L)$ velocity of the plate, L: characteristic length of the plate, $\bar{u}_{slip} = N_1\, v\frac{\partial \bar{u}}{\partial \bar{y}}$: linear slip velocity, N_1 velocity slip factor with dimension s/m, ρ_f: density of the base fluid, σ: electric conductivity, μ: dynamic viscosity of the base fluid, ρ_P : density of the nanoparticles, $(\rho Cp)_f$: effective heat capacity of the fluid, $(\rho Cp)_p$ effective heat capacity of the nanoparticle material, Q_0 volumetric rate of heat generation/absorption, ε: porosity, D_B : Brownian diffusion coefficient, D_T : thermophoretic diffusion coefficient and q_r: radiative heat transfer in $\bar{y}$-direction. We consider the fluid to be a gray, absorbing-emitting but non scattering medium. We also assume that the boundary layer is optically thick and the Rosseland approximation or diffusion approximation for radiation is valid [30,31]. Thus, the radioactive heat flux for an optically thick boundary layer (with intensive absorption), as elaborated by Sparrow and Cess [32,33] defined as $q_r = (\frac{-4\sigma_1}{3k_1})(\partial T^4/\partial\, \bar{y})$ where σ_1 (=5.67X $10^{-8} W/m^2 K^4$) is the Stefan-Boltzmann constant and $k_1(m^{-1})$ Rosseland mean absorption coefficient. Purely analytical solutions to the partial differential boundary value problem defined by (2)–(4) are not possible. Even a numerical solution is challenging. Hence we aim to transform the problem to a system of ordinary differential equations. We define the following dimensionless transformation variables:

$$\eta = \frac{\bar{y}}{\sqrt{K_p}},\ \psi = U_r(\bar{x}/L)\sqrt{K_p}f(\eta),\ \theta(\eta) = \frac{T - T_\infty}{T_f - T_\infty},\ \varphi(\eta) = \frac{C - C_\infty}{C_f - C_\infty}, \tag{6}$$

where L is the characteristic length. From (4), we have $T = T_\infty\{1 + (T_r - 1)\theta\}$, where $T_r = T_f/T_\infty$ (the wall temperature excess ratio parameter) and hence $T^4 = {T^4}_\infty\ \{1 + (T_r - 1)\theta\}^4$. Substitution of (6) into (2)-(4) generates the following similarity equations:

$$f''' + Re\ Da\ (ff'' - f'^2 - M\,f') - f' = 0 \tag{7}$$

$$\theta'' + Re\,\mathrm{Pr}\,Da\,f\,\theta' + \mathrm{Pr}\left[Nb\,\theta' f\varphi' + Nt\,\theta'^2\right] + \frac{4}{3R}[\{1+(T_r-1)\theta\}^3\theta']' + Q\theta = 0 \tag{8}$$

$$\varphi'' + Re\,\mathrm{Le}\,Da\,f\,\varphi' + \frac{Nt}{Nb}\,\theta'' - \gamma\,\varphi = 0 \tag{9}$$

The relevant boundary conditions are

$$f(0) = 0\,, f'(0) = 1 + a\,f''(0), f'(\infty) = 0\,,$$

$$\theta'(0) = -Nc[1-\theta(0)], \theta(\infty) = 0$$

$$\varphi'(0) = -Nd[1-\varphi(0)], \varphi(\infty) = 0 \tag{10}$$

where primes denote differentiation with respect to η. The thermo physical dimensionless parameters arising in (7)–(9) are defined as follows: $Re = U_r L/v$ is the Reynolds number, $Da = k_p/L^2$ is the Darcy number, $M = \sigma B_0^2\, L\, /U_r\,\rho$ is the magnetic field parameter, $Pr = v/\alpha$ is the Prandtl number, $Nt = \tau D_T(T_f - T_\infty)/vT_\infty$ is the thermophoresis parameter, $Nb = \tau D_B(C_f - C_\infty)/v$ is the Brownian motion parameter, $R = kk_1/4\sigma_1 T_\infty^3$ is the convection-radiation parameter, $Le = v\ /D_B$ is the Lewis number, $a = N_1 v/\sqrt{K_p}$ is the hydrodynamic (momentum) slip parameter, $Nd = h_m\sqrt{K_p}\ /D_B$ is the convection-diffusion parameter, $Nc = h_f\sqrt{K_p}/k$ is the convection-conduction parameter and the chemical reaction parameter $\gamma = k_c(C - C_\infty)$. Quantities of physical interest are the local friction factor, $C_{f_{\bar{x}}}$, the local Nusselt number, $Nu_{\bar{x}}$ and the local Sherwood number, $Sh_{\bar{x}}$. Physically, C_{f_x} represents the wall shear stress, $Nu_{\bar{x}}$ defines the heat transfer rates and $sh_{\bar{x}}$ defines the mass transfer rates:

$$C_{f_x}\,Re_x^{-1}\,Da_x^{0.5} = 2f''(0)\,,\quad Sh_{\bar{x}}\ Da_{\bar{x}}^{0.5} = -\varphi'(0)$$

$$Nu_{\bar{x}}\ Da_{\bar{x}}^{0.5} = -[1+\tfrac{4}{3R}\{1+(T_r-1)\theta(0)\}^3]\theta'(0) \tag{11}$$

3 Results and Discussion

The numerical simulation of equations (7)-(9) subject to the boundary condition (10) are carried out for various values of the physical parameters such as Reynolds number *Re*, magnetic field parameter *M*, Prandtl number *Pr*, thermophoresis parameter *Nt*, Brownian motion parameter *Nb*, convection-radiation parameter *R*, Lewis number *Le*, hydrodynamic (momentum) slip parameter *a*, convection-diffusion parameter *Nd*, convection-conduction parameter *Nc*. In order to get a physical understanding of the problem the results have been performed for the velocity, temperature and concentration profiles. The results are presented graphically in Figs. 1-10. The effect of Reynolds number *Re* is shown in Fig. 1(a)-1(c), respectively, for velocity, temperature and concentration profiles which demonstrates that the increase of Reynolds number enhanced the fluid velocity in core region of saturated porous medium in the case of no-slip boundary conditions and slip boundary conditions. It is also noticed that the velocity gradient at the interface increases with the increase of Reynolds number *Re*. It is also found that the velocity profiles decrease with the increasing of velocity parameter. Both the temperature and concentration profiles decreases with the increase of Reynolds number *Re*. From Fig. 1(b), it is also noticed that with the increase of conduction-convection parameter *Nc*, the temperature profiles increases. Fig. 1(c) also demonstrates that the concentration profiles decreases with the increase of convection-diffusion parameter *Nd*.

Fig. 2(a) to 2(c) illustrate the velocity, temperature and concentration profiles for different values of heat source/sink parameter Q. From Fig. 2(a), it revel that with the effect of heat source/sink parameter (Q<0), the velocity profiles decreases and the velocity profiles increase with heat source (Q>0). There is a significant variation is observed from Fig. 2(b) the temperature profiles decreases with heat source/sink parameter (Q<0) on the contrary, the temperature profiles increases with heat source/sink (Q>0) for both cases with and

without convection-conduction parameter *Nc*. Fig. 2(c) represents the effect of heat source/sink parameter *Q*, for different values of convection diffusion parameter *Nd* on concentration profiles. The concentration profiles increase in case of heat source/sink *Q<0,* while the concentration profiles decreases with heat source/sink parameter Q>0. It is interested to note that the heat sources effect is higher for higher conduction-diffusion parameter *Nd*. Therefore, the thermal and concentration boundary layer thickness are enhanced. Fig. 3 depicts the influence of chemical reaction on the dimensionless temperature and solutal concentration profiles with the fixed values of other parameters. It is obvious that an increase in the chemical reaction parameter results a decreasing in the solutal concentration profile. The distribution of solutal concentration becomes weak in the presence of chemical reaction. So, the solutal concentration boundary layer becomes thin as the chemical reaction parameter increases. From Fig. 3, it is observed that the chemical reaction influences the solutal concentration field. However, it has a minor effect on thermal diffusion. This explains the minor influence of chemical reaction on temperature profile. It is worth mentioning here that, the large values of γ shows small changes on temperature field.

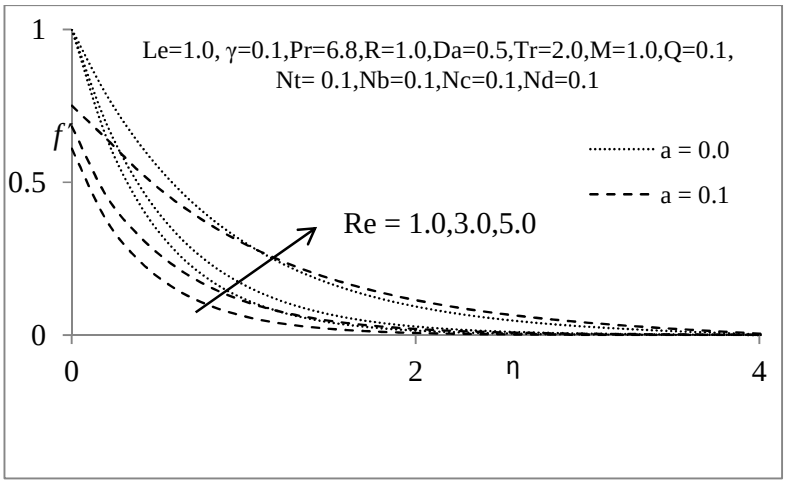

Fig. 1a. Velocity profiles for various values of *Re*

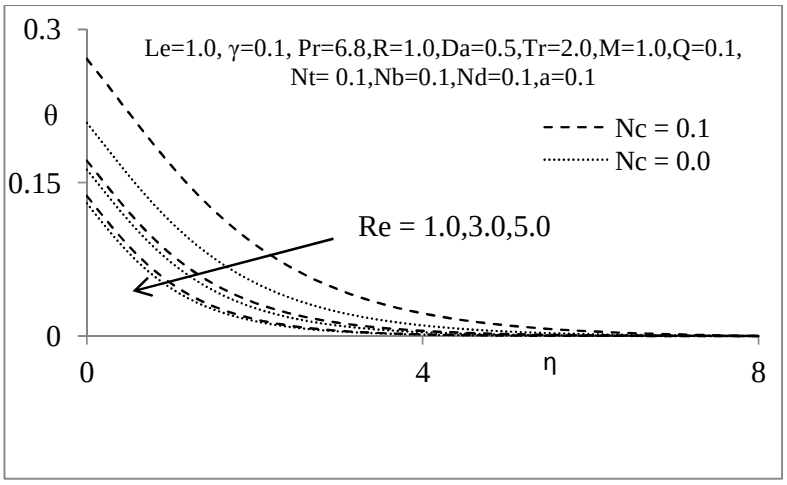

Fig. 1b. Temperature profiles for various values of *Re*

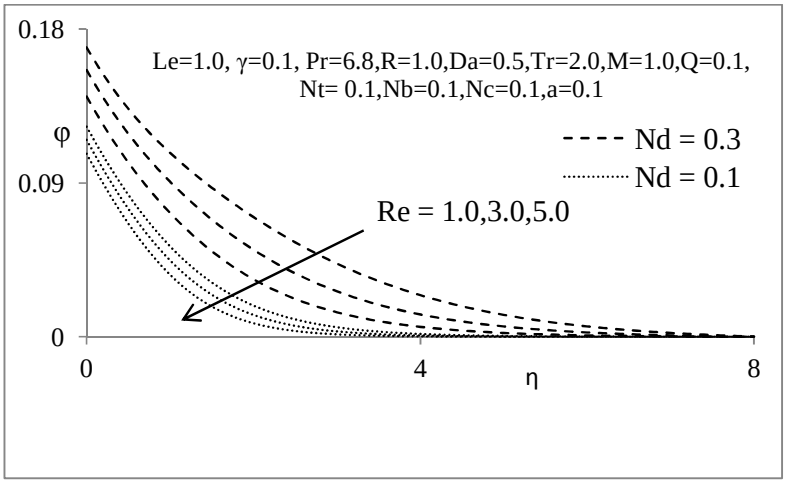

Fig. 1c. Concentration profiles for various values of *Re*

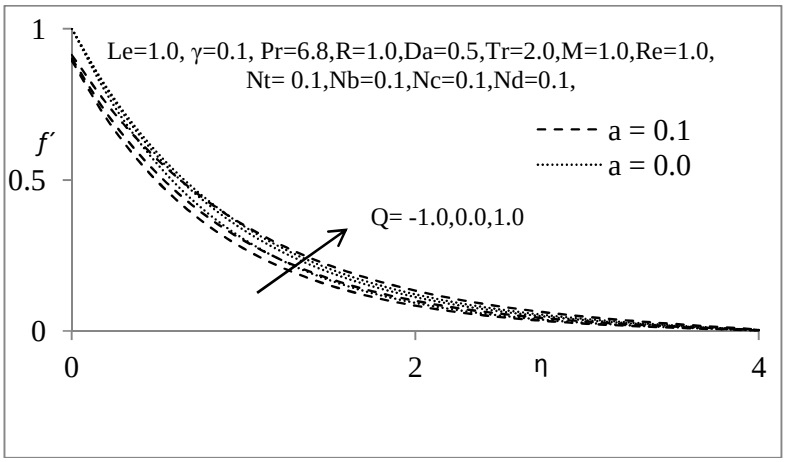

Fig. 2a. Velocity profiles for various values of Q

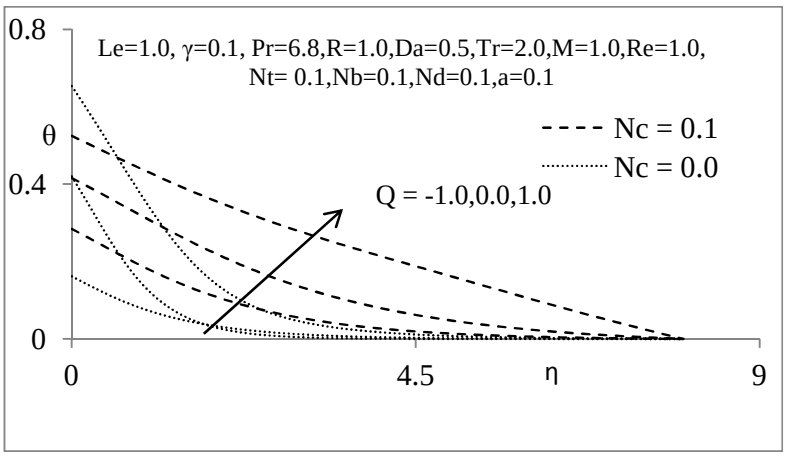

Fig. 2b. Temperature profiles for various values of Q

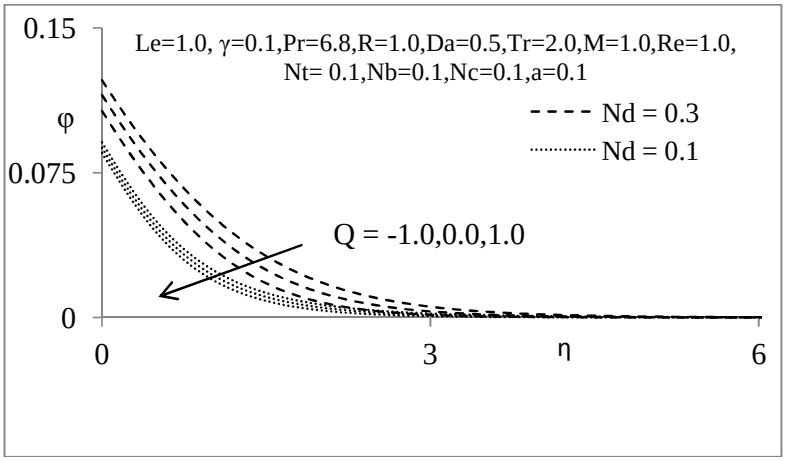

Fig. 2c. Concentration profiles for various values of Q

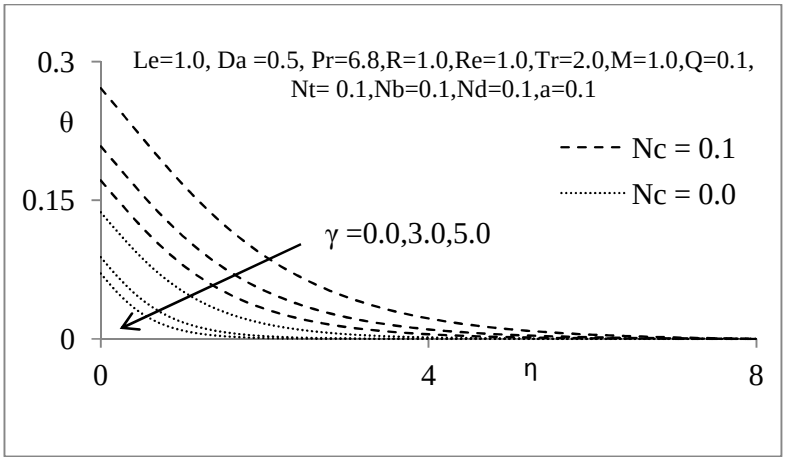

Fig. 3a. Temperature profiles for various values of *Da*

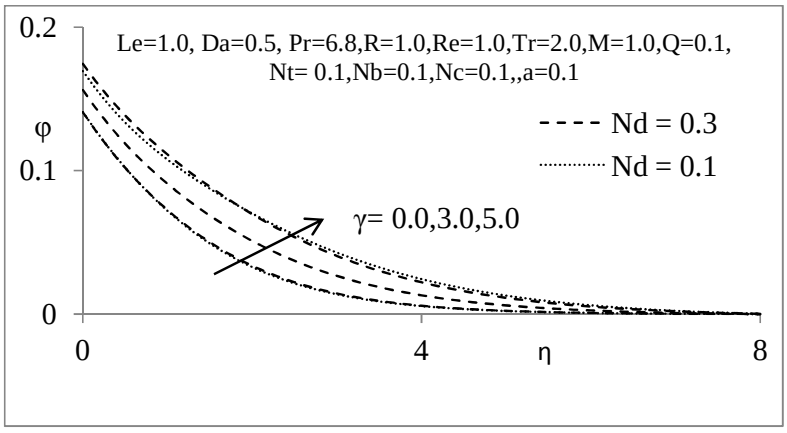

Fig. 3b. Concentration profiles for various values of *Da*

The velocity, temperature and concentration display in 4(a) and 4(b). It is depicted that the effect of magnetic fluid is to decrease the velocity field for the cases slip and no slip boundary conditions. It is due to Lorentz forces in the saturated porous medium. When the strength of the magnetic field increase the velocity gradient at the interface has been diminishes, the temperature profiles increases with the increase of magnetic field *M*. Fig. 5(a) and 5(b) demonstrates that an increase Chemical reaction parameter γ increases velocity as well as temperature profiles. It can be also noticed that the convection parameter *Nc* increases the temperature profiles. Fig. 6(a) and 6(b) depict the influence of thermal radiation parameter *R* on velocity and temperature profiles. It can be seen from the figure that the velocity profiles increase with the increase of Reynolds number *Re*, while the temperature profiles with the increase of *R*. This is due to the Radiation term appeared in equation (8) is inversely proportional to the radiation parameter *R*. Thus, small *R* signifies a large radiation effect while *R* tends to infinite correspond to no radiation effect. Evidently the presence of thermal radiation flux is demonstrated to heat the thermal boundary layer significantly and is benefited to material characteristic. Fig. 7 displays the effect of Prandtl number *Pr* for the cases without biot number *Nc = 0* and with the effect of biot number *Nc=0.1*, it is worth mentioning that the temperature profiles decrease with the increase of Prandtl number *Pr*. From Fig. 8, it is evident that the effect of Lewis number *Le* leads to decrease the concentration profiles. Fig. 9, represents the effect of thermophorasis parameter *Nt* when conduction parameter *Nc=0*(without biot number), *Nc= 0.1*(with biot number) with influence of thermophorasis parameter *Nt*. The concentration profiles increase with increase of thermophorasis parameter *Nt*. It is worth mentioning that the thermophorasis parameter *Nt* effect is more in the presence of Biot number *Nc*. The effect of Brownian motion parameter *Nb* is to display on concentration profiles in Fig. 10. It can be seen that the Brownian motion parameter *Nb* effects lead to decrease the concentration profiles. It is evident from Fig. 11, the variation of skin fraction parameter $f''(0)$ decreases with the increase of radiation parameter *R* and increases with the increase of magnetic parameter *M*. The Fig. 12 is done for the values of $\theta'(0)$ verses the magnetic field parameter *M*. From figure it revealed that the heat transfer coefficient $\theta'(0)$ is to increase with the increase of *R* and reduces the values with increase of values of magnetic parameter *M*. Fig. 13 is plotted for the Sherwood number $\varphi'(0)$ verses the magnetic parameter *M* for different values of radiation parameter *R*. The results indicate that an increasing magnetic parameter *M* is to decrease the Sherwood parameter coefficients $\varphi'(0)$ values. It is also noticed that the Sherwood parameter coefficients $\varphi'(0)$ values increasing with the increase of radiation parameter *R*.

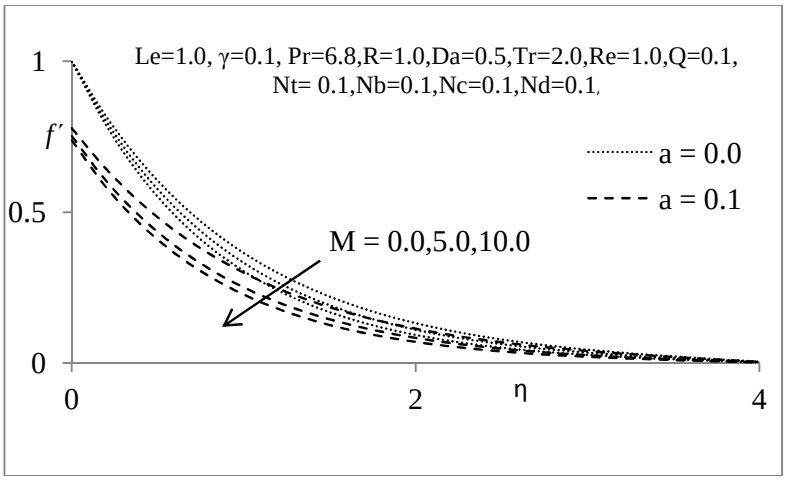

Fig. 4a. Velocity profiles for various values of *M*

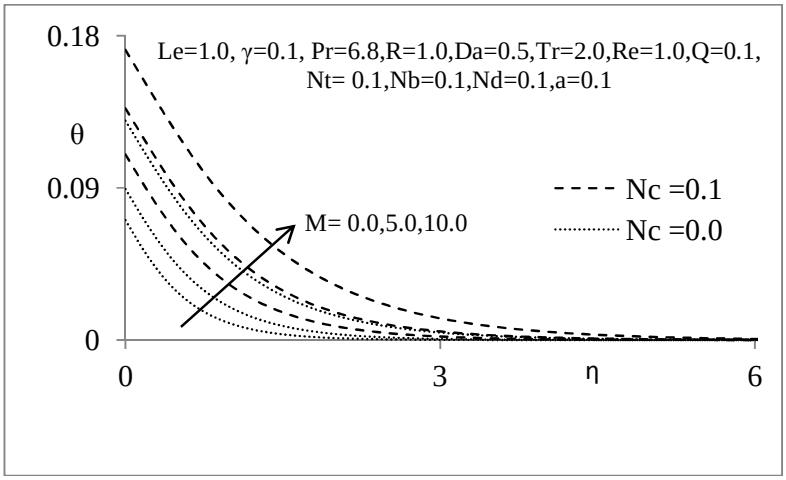

Fig. 4b. Temperature profiles for various values of M

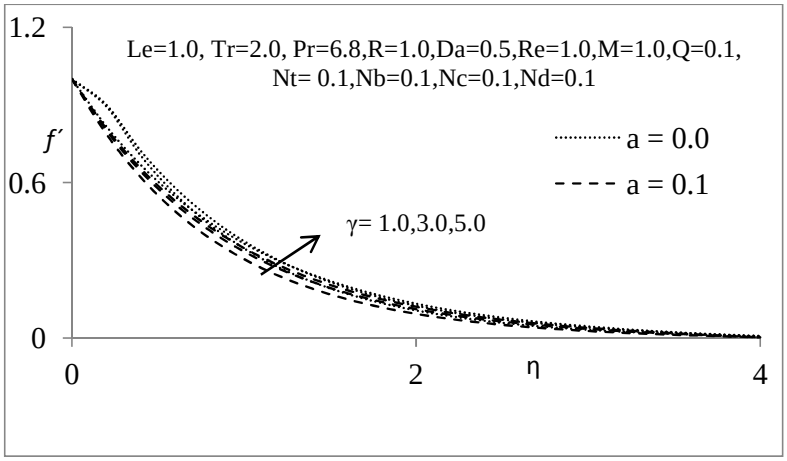

Fig. 5a. Velocity profiles for various values of γ

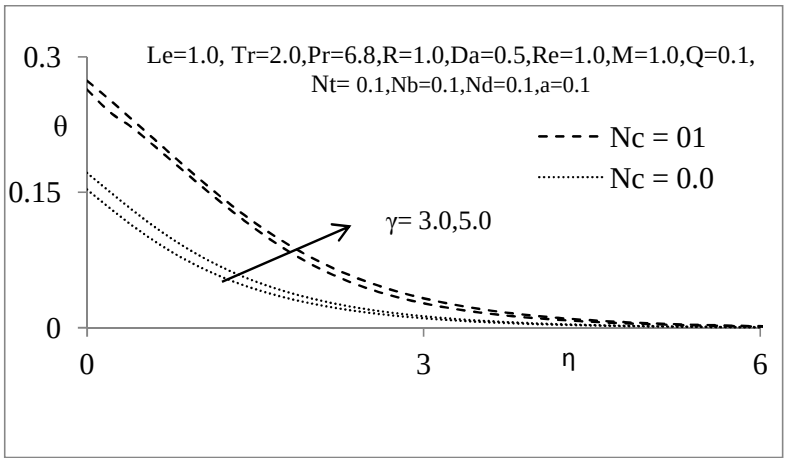

Fig. 5b. Temperature profiles for various values of γ

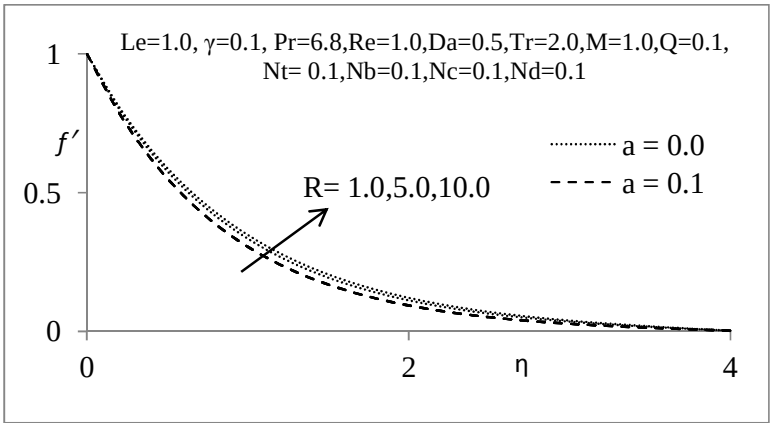

Fig. 6a. Velocity profiles for various values of *R*

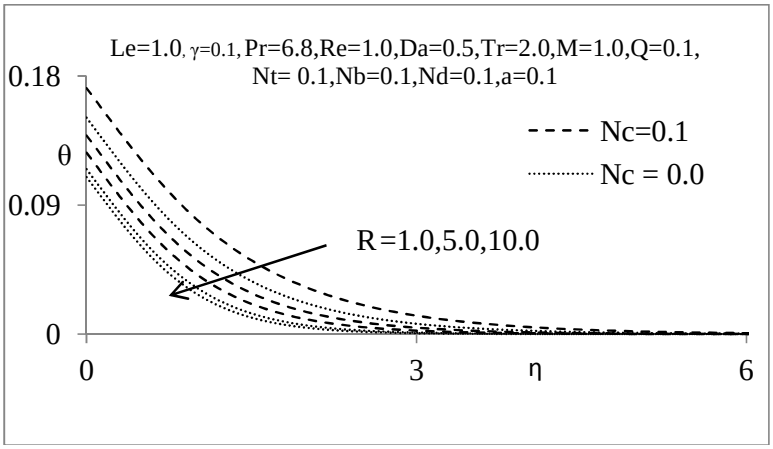

Fig. 6b. Temperature profiles for various values of *R*

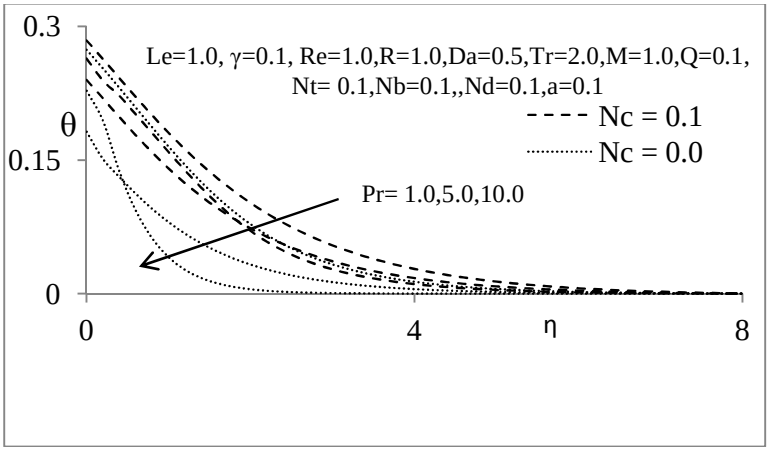

Fig. 7. Temperature profiles for various values of *Pr*

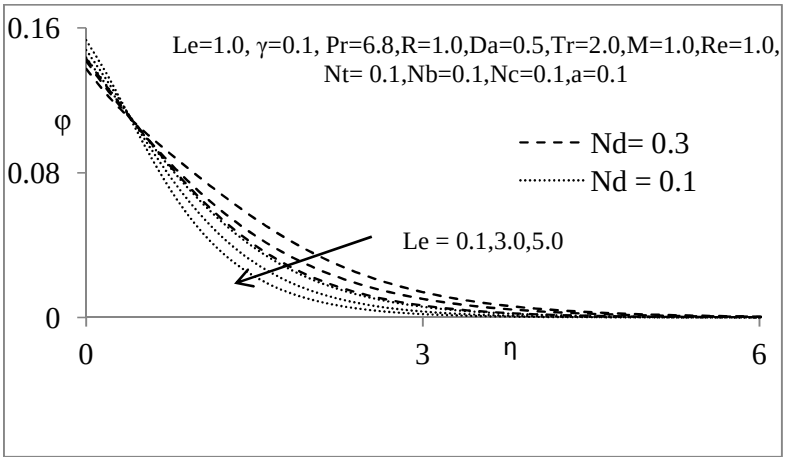

Fig. 8. Concentration profiles for various values of Le

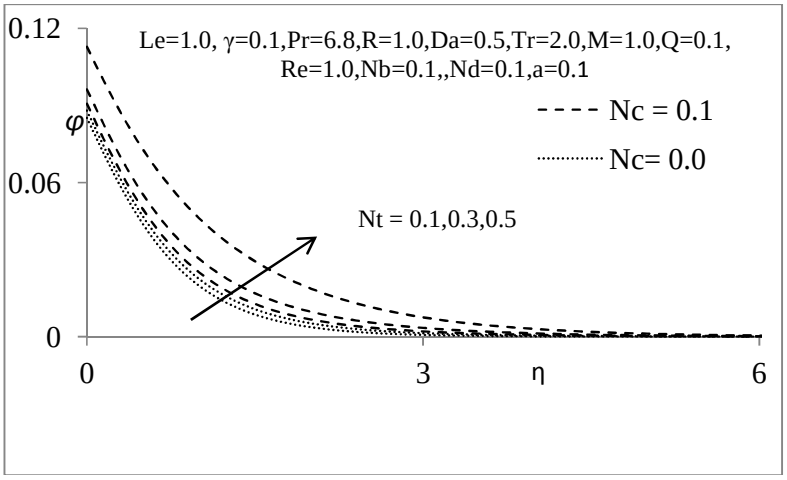

Fig. 9. Concentration profiles for various values of Nt

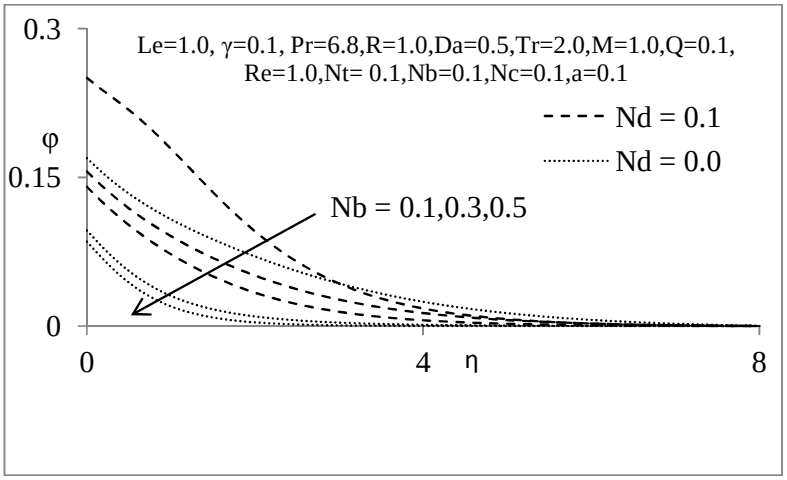

Fig. 10. Concentration profiles for various values of Nb

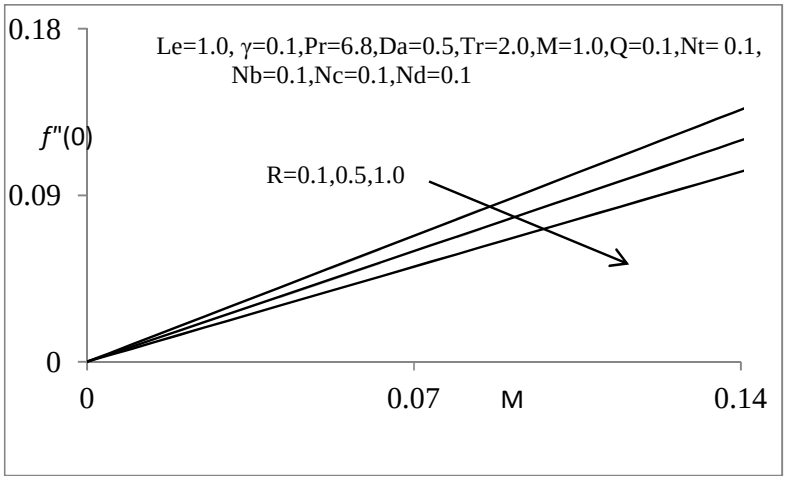

Fig. 11. Variation of Skin-frication for different values of R

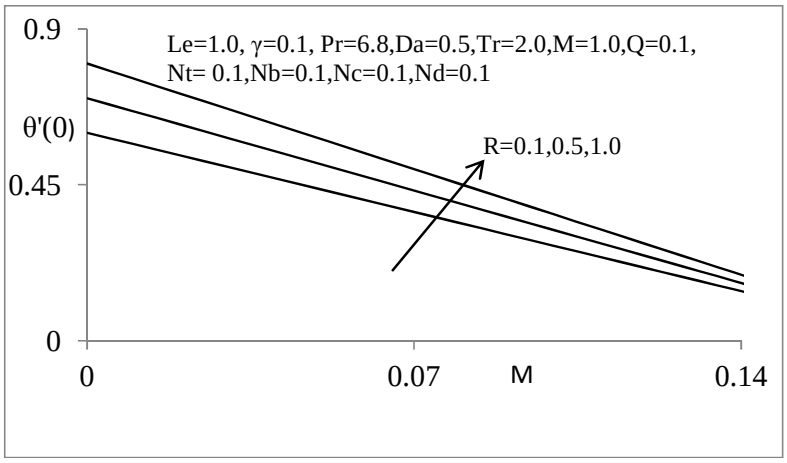

Fig. 12. Distribution of heat transfer at the channel wall for different values of R

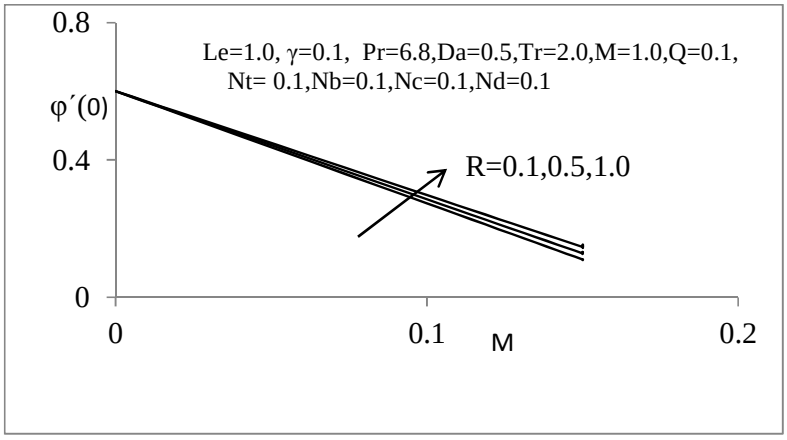

Fig. 13. Distribution of the rate of concentration at the channel wall for different values of R

4 Conclusion

In the present investigation, an analysis in order to study the chemical reaction effects of magnetohydrodynamics convection slip flow of a thermosolutal nanofluid in a saturated porous media over a radiating stretching sheet with heat source/sink. In this study the density is dependent on velocity, temperature and concentration profiles. The governing equations are transformed to the high non-linear ordinary differential equations by the use of similarity transformation and are solved analytically using finite difference method along with the Gauss-seidel method. The physical parameters such as Reynolds number, chemical reaction parameter, magnetic field parameter, Prandtl number, thermophoresis parameter, Brownian motion parameter, convection-radiation parameter, Lewis number, hydrodynamic (momentum) slip parameter, convection-diffusion parameter, convection-conduction parameter on velocity, temperature and concentration profiles are depicted and discussed in this paper.

Competing Interests

Authors have declared that no competing interests exist.

References

[1] Buongiorno J, Hu W. Nanofluid coolants for advanced nuclear power plants. Proceedings of the International Congress on Advances in Nuclear Power Plants (ICAPP ’05), Paper no. 5705, Seoul, Korea; 2005.

[2] Buongiorno J. Convective transport in nanofluids. Journal of Heat Transfer. 2006;128(3):240–250.

[3] Dulal Pal, Netai Roy, Lie Group. Transformation on MHD radiative dissipative casson nanofluid flow over a vertical non-linear, stretching surface with non-uniform heat source/sink and chemical reaction. J. Nanofluids. 2016;5:839–851.

[4] Jamalabadi MYA. Entropy generation in boundary layer flow of a micro polar fluid over a stretching sheet embedded in a highly absorbing medium. Frontiers in Heat and Mass Transfer (FHMT). 2015;6 (1).

[5] Afify AA, Uddin MJ, Ferdows M. Scaling group transformation for MHD boundary layer flow over permeable stretching sheet in presence of slip flow with Newtonian heating effects. Applied Mathematics and Mechanics. 2014;35(11):1375–1386.

[6] Vafai K (Ed.). Handbook of porous media. Second ed. Taylor & Francis, New York; 2005.

[7] Pop I, Ingham DB. Convective heat transfer: Mathematical and computational modelling of viscous fluids and porous media. Pergamon, Oxford; 2001.

[8] Bejan A, Dincer I, Lorente S, Miguel AF, Reis AH. Porous and complex flow structures in modern technologies. Springer, New York; 2004.

[9] Choi S. Enhancing thermal conductivity of fluids with nanoparticles. Developments and applications of non-Newtonian flows. Presented at the ASME International Mechanical Engineering Congress and Exposition, November 12–17, San Francisco, Calif, USA. D. A. Siginer and H. P. Wang, Eds. ASME. 1995;231. 1995;66:99–105.

[10] Chamkha AJ, Alymhd AM. Free convection flow of a nanofluid past a vertical plate in the presence of heat generation or absorption effects. Chem. Eng. Comm. 2011;198:425-441.

[11] Muthucumaraswamy R. Chemical reaction effects on vertical oscillating plate with variable temperature. Chem. Ind. Chem. Eng. Quart. 2012;16:167-173.

[12] Muthucumaraswamy R, Manivannan K. First order chemical reaction on isothermal vertical oscillating plate with variable mass diffusion. Int. J. Pure Appl. Sci. Technol. 2011;3:19-26.

[13] Chamkha AJ, Issa C. Effects of heat generation or absorption and thermophoresis on hydromagnetic flow with heat and mass transfer over a flat surface. Int. J. Numer. Method. Heat. Fluid Flow. 2000; 10:432-449.

[14] Srinivas Maripala, Kishan N. Unsteady MHD flow and heat transfer of nanofluid over a permeable shrinking sheet with thermal radiation and chemical reaction. American Journal of Engineering Research. 2015;4(6):01-12.

[15] Makinde OD, Aziz A. Boundary layer flow of a nanofluid past a stretching sheet with a convective boundary condition. Int. J. Therm. Sci. 2011;50:1326-1332.

[16] Srinivas Maripala, Kishan Naikoti. MHD Mixed convective heat and mass transfer through a stratified nanofluid flow over a thermal radiative stretching cylinder. International Journal of Mathematics Research. 2016;5(1):40-57.

[17] Srinivas Maripala, Kishan Naikoti. MHD effects on micropolar nanofluid flow over a radiative stretching surface with thermal conductivity. Advances in Applied Science Research. 2016;7(3):73-82.

[18] Hunegnaw Dessie, Naikoti Kishan. MHD effects on heat transfer over stretching sheet embedded in porous medium with variable viscosity, viscous dissipation and heat source/sink. Ain Shams Engineering Journal. 2014;5(3):967-977.

[19] Aziz A. A similarity solution for laminar thermal boundary layer over a flat plate with a convective surface boundary condition. Communications in Nonlinear Science and Numerical Simulation. 2009;14(4):1064–1068.

[20] Ali N, Khan SU, Abbas Z, Sajid M. Soret and Dufour effects on hydromagnetic flow of viscoelastic fluid over porous oscillatory stretching sheet with thermal radiation. Journal of the Brazilian Society of Mechanical Sciences and Engineering. 2016;38:2533-2546.

[21] Sami Ullah Khan, Nasir Ali, Zaheer Abbas. MHD flow and heat transfer over a porous oscillating stretching surface in a viscoelastic fluid with porous medium. Plos One. 2015;10(12):e0144299.

[22] Nasir Ali, Sami Ullah Khan, Muhammad Sajid, Zaheer Abbas. MHD flow and heat transfer of couple stress fluid over an oscillatory stretching sheet with heat source/sink in porous medium. Alexandria Engineering Journal. 2016;55:915–924.

[23] Khan Sami Ullah, Ali Nasir Abbas. Zaheer influence of heat generation/absorption with convective heat and mass conditions in unsteady flow of eyring powell nanofluid over porous oscillatory stretching surface. Journal of Nanofluids. 2016;5(3):351-362.

[24] Kishan N, Kavitha P. Effects of heat source/sink on MHD flow and heat transfer of a non-Newtonian power-law fluid on a stretching surface with thermal radiation and slip-conditions. Thermal Science. 2014;35-35.
DOI: 10.2298/tsci130616035n

[25] Srinivas Maripala, Kishan Naikoti. MHD convection slip flow of a thermosolutal nanofluid in a saturated porous media over a radiating stretching sheet with heat source/sink. Advances and Applications in Fluid Mechanics. 2015;18(2):177.

[26] Buongiorno J. Convective transport in nanofluids. Journal of Heat Transfer. 2006;128(3):240–250.

[27] Makinde OD, Aziz A. Boundary layer flow of a nanofluid past a stretching sheet with a convective boundary condition. International Journal of Thermal Sciences. 2011;50(7):1326–1332.

[28] Datta AK. Biological and bioenvironmental heat and mass transfer. Marcel Dekker, New York, NY, USA; 2002.

[29] Karniadakis G, Beskok A, Aluru N. Microflows and nanoflows fundamentals and simulation. Springer Science, New York, NY, USA; 2005.

[30] Cortell R. Effects of viscous dissipation and radiation on the thermal boundary layer over a nonlinearly stretching sheet. Physics Letters A: General, Atomic and Solid State Physics. 2008;372(5):631–636.

[31] B´eg OA, Zueco J, B´eg TA, Takhar HS, Kahya E. NSM analysis of time-dependent nonlinear buoyancy-driven double diffusive radiative convection flow in non-Darcy geological porous media. Acta Mechanica. 2009;202(1–4):181–204.

[32] Sparrow EM, Cess RD. Radiation heat transfer, chapters 7 & 10, Hemisphere, Washington, DC, USA.

[33] Dayyan M, Seyyedi SM, Domairry GG, Gorji Bandpy M. Analytical solution of flow and heat transfer over a permeable stretching wall in a porous medium. Mathematical Problems in Engineering. 2013;Article ID 682795:10.

Peer-review history:
The peer review history for this paper can be accessed here (Please copy paste the total link in your browser address bar)
http://sciencedomain.org/review-history/17422